STRENGTH AND ELASTICITY OF IRON AND COPPER AT HIGH SHOCK-WAVE COMPRESSION PRESSURES

L. V. Al'tshuler, M. I. Brazhnik,* and G. S. Telegin

UDC 539.32+539.411.5

The elastic and strength parameters of iron and copper were determined experimentally at high shock-wave compression pressures of 1-2 Mbar. The attenuation of shock waves created by the impact of thin plates in blocks of the investigated materials was recorded in the experiments. The Poisson ratios, bulk moduli, shear moduli, and yield strength Y for iron at 1.11 and 1.85 Mbar and for copper at 1.22 Mbar were determined from the experimentally observed amplitudes and velocites of the unloading shock waves. The shape of the curve of the change of the yield strength of copper with an increase of pressures to states of shock-wave compression causing melting was determined on the basis of the results obtained and data of other investigators. The curve has a maximum at $P \sim 800$ kbar corresponding to $Y = 280$ kg/mm^2. The yield strengths for iron are located on the ascending branch of the curve Y(P) and are numerically equal to 110 kg/mm^2 at 1.11 Mbar and 270 kg/mm^2 at 1.85 Mbar. The measured values of Y exceed the yield strengths of uncompressed metals by a factor of 5-7. The authors also recorded a substantial increase of Poisson's ratios with increase of pressures in the investigated metals.

This article presents the results of a determination of the strength and elasticity of copper and mild steel (0.2%C) behind the front of strong shock waves. To obtain the necessary experimental information on the elasticity and strength of solids at high shock-wave pressures, we conducted observations of the expansion of the specimens after their shock-wave compression. As was shown for the first time experimentally in [1], unloading of shock-wave compressed metals occurs in two stages. In the first stage it is accomplished by one-dimensional elastic waves, and in the second stage – the field of transition of the material to a plastic state – by plastic three-dimensional deformation waves propagating with smaller velocities. By means of the same method as in [1], which is based on a study of the attenuation of waves created by the impact of thin plates, in subsequent studies the amplitudes of the unloading elastic waves were determined and the critical shear stresses were estimated in aluminum [2-6] in the pressure range from 300 to 680 kbar and in copper [6] at pressures of 340 and 860 kbar. In the investigation to be presented the strength and elastic characteristics of copper and iron are found at even higher pressures, 1-3 Mbar.

The elastoplastic model of the medium used and the schemes of shock-wave loading and unloading necessary for interpreting the results obtained are presented in the first section of the article. Experimental data are given in the second section. The third section is devoted to their subsequent treatment and discussion.

1. Schemes of One-Dimensional Elastoplastic Deformation. In a macroscopic consideration a substance during passage of shock waves experiences one-dimensional deformation in the direction of travel

*Deceased.

Moscow. Translated from Zhurnal Prikladnoi Mekhaniki i Tekhnicheskoi Fiziki, No. 6, pp. 159-166, November-December, 1971. Original article submitted March 20, 1970.

TABLE 1

Series	Metal	D, km/sec	U, km/sec	p_n, Mbar	ρ/ρ_0	T, °K	Δp_n, kbar	l_e/Δ	C_e, km/sec
I	Fe	8.39	2.81	1.850	1.503	4400	210±35	3.67±0.10	9.75±0.2
II	Fe	7.075	2.00	1.110	1.394	2500	80±20	4.13±0.10	8.32±0.15
III	Cu	6.90	1.98	1.220	1.402	2300	100±20	4.40±0.10	7.81±0.15

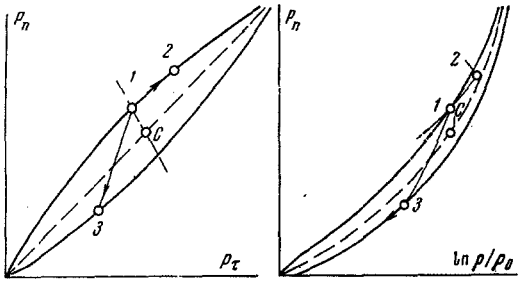

Fig. 1

of the wave front. The deformations are equal to zero in perpendicular directions lying in the plane of the wave front. Expansion of a substance in plane unloading waves has the same character.

In elastic phases of compression and expansion the relation between the stress components and average pressure in the presence of one-dimensional deformation is established by the relationships

$$dp_\tau = \frac{\sigma}{1-\sigma} dp_n, \quad 3p = p_n + 2p_\tau \tag{1.1}$$

which follow directly from Hooke's law. Here p_n is compressive stress in the direction of strain; the p_τ are the compressive stresses in perpendicular directions; p is the "hydrostatic" pressure; σ is Poisson's ratio.

In the plastic state the values of the components satisfy the plasticity condition

$$p_n - p_\tau = \pm Y(p, T) \tag{1.2}$$

which takes into account the dependence of the yield strength Y both on pressure and on temperature T.

The behavior of elastoplastic materials during shock-wave compression and subsequent expansion according to [7, 8] is shown schematically in the diagrams of Fig. 1. The stress components p_n and p_τ are laid out along the axes in Fig. 1a. The inclined solid lines of the diagram represent sections of the boundary surfaces satisfying Eq. (1.2). Since the yield strength depends on temperature, the shape of the boundary surfaces is different for different thermodynamic processes. For states situated near the adiabatic curve the interval between the boundary surfaces at first increases with amplitude of the shock wave under the effect of pressures, and then decreases as the temperature of shock-wave compression increases, vanishing upon melting of the substance.

According to traditional concepts, at shock-wave compression pressures exceeding the Hugoniot elastic limit the characteristics of the medium correspond to states of the upper boundary surface of plastic flow. Under these conditions the behavior of the medium with respect to the direction of further deformation is asymmetric. For "positive" deformations coinciding in sign with the preceding deformation of the shock passage the characteristic point of the state moves away from the origin of the coordinates, retaining its position on the surface of plastic flow (line 1-2). In the case of "negative" deformation of expansion an elastic unloading stage is realized along isentrope 1-3, which is completed with arrival of the characteristic point on the lower boundary surface. On the basis of Eqs. (1.1) and (1.2) the maximum amplitude of the unloading shock wave is

$$p_1 - p_3 = \Delta p_n = 2\frac{1-\sigma}{1-2\sigma} Y \tag{1.3}$$

An alternative hypothesis is that hydrostatic states located along the bisector of a right angle, along the midline of the elastic zone, occur behind the shock front as a result of relaxation processes taking place at the front. This hypothesis, requiring experimental substantiation, reduces the maximum amplitude of the unloading elastic waves by half in comparison with (1.3).

The relative position of the elastic and "plastic" isentropes and the Hugoniot adiabatic curve are shown schematically in Fig. 1b. The normal component p_n is plotted along the y axis and the natural logarithms of the ratio of the current value of density ρ to its initial value ρ_0 are laid out along the x axis. In these variables the slopes of the curves characterize the bulk moduli (reciprocals of compressibility) of the me-

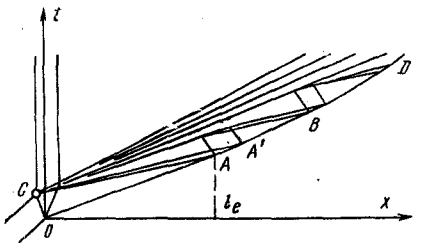

Fig. 2

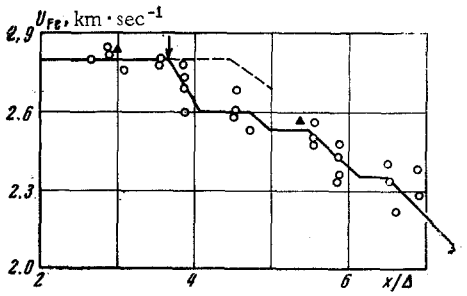

Fig. 3

dium. Three curves important for further consideration intersect state 1 of shock-wave compression: isentrope 1-2(p_S) with bulk modulus

$$K_S = \rho C_S^2 \tag{1.4}$$

curve 1-3 of one-dimensional elastic expansion (p_{Se}), having modulus

$$K_e = \rho C_e^2 = \frac{3(1-\sigma)}{1-2\sigma} K_S \tag{1.5}$$

and the shock adiabatic curve $p_H(\rho)$. Its modulus $K_H = dp_n/d \ln \rho$ according to [9, 10] is related with (1.4) by a thermodynamic identity

$$2K_S = \gamma [(1 + 2\gamma^{-1} - \rho\rho_0^{-1}) K_H + p_H] \tag{1.6}$$

In Eqs. (1.4)-(1.6) C_S is the plastic sound velocity, i.e., the propagation velocity of weak volume disturbances; C_e is the propagation velocity of one-dimensional elastic deformations, or the elastic sound velocity; γ is the Gruneisen gamma, equal to the ratio of thermal pressure to thermal energy density.

Experiments on shock-wave compression of solid and porous specimens of investigated materials yield the necessary information both on the Gruneisen gamma and on the slopes of the dynamic adiabatic curves. If in wave velocity D versus mass velocity U coordinates the shock adiabatic curve is given on some segment by the linear relation

$$D = C_0 + \lambda U \tag{1.7}$$

its modulus is

$$K_H = \rho (D + \lambda U) (D - U)^2 C_0^{-1} \tag{1.8}$$

For known K_H and γ Eq. (1.6) can be used for calculating the isentropic bulk modulus K_S. We note that it can be found also on the basis of the sound velocity C_S, as was done in [1].

The search for the modulus of one-dimensional elastic deformation K_e, Poisson's ratio σ, and dynamic yield strength Y, as follows from Eqs. (1.3) and (1.5), requires independent additional experimental measurements of the propagation velocities C_e and amplitudes Δp_n of the unloading elastic waves.

2. Experimental Method and Results. To determine C_e and Δp_n we used the "overtaking unloading method" [1], which is based on a study of attenuation in the investigated material of the shock waves arising upon impact of thin plates. In the simplest variant of the method the striking plates and specimens are made of the same material.

As we see from the path x versus time t diagram (Fig. 2), shock waves OC and OAA'BD propagate from the site of collision O along the specimen and striker. At the moment of arrival of the shock wave on the rear surface of the striker a centered elastoplastic unloading wave occurs at point C which overtakes the shock wave and causes its attentuation. The arrival of the front of the unloading elastic wave at the trajectory of the shock wave occurs at distance

$$l_e = \frac{1+M}{1-M} \Delta \tag{2.1}$$

where Δ is the thickness of the striking plate and $M = (D-U)/C_e$ is the Mach number for the elastic wave. Equation (2.1) permits, having revealed the place of overtaking, finding M and consequently the velocity of the elastic wave C_e for known values of velocities D and U. In turn the amplitude Δp_n of the unloading elastic wave is found from the decrease of pressures on the unloaded section of the trajectory A'B.

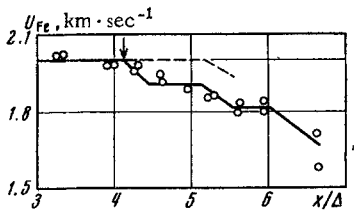

Fig. 4

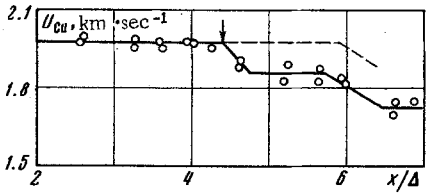

Fig. 5

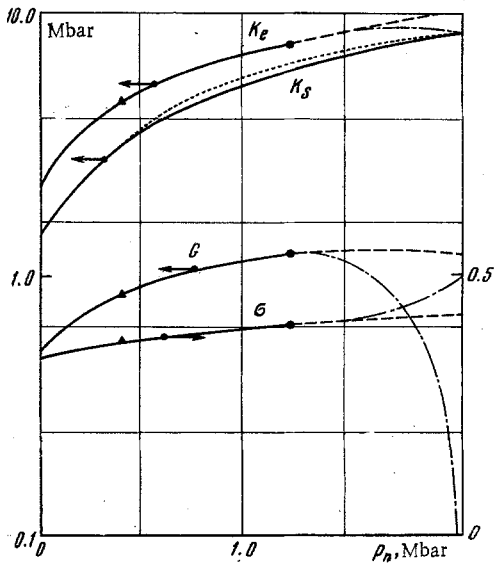

Fig. 6

Numerous experiments were carried out for an experimental determination of distance-varying amplitudes of shock waves on specimens – obstacles of different thickness. The amplitude of the wave at a given distance from the collision surface, as in [1], was found from the velocity of a thin (0.15 mm) aluminum plate placed on the free surface of the obstacle. As an analysis of the propagation of shock waves and unloading waves along the plate showed, the velocity of the plate characterizes the state of the shock front at a distance of about 0.2 mm from its boundary with the specimen. The times and consequently the velocities of the plates were recorded on a high-speed moving-image camera on the basis of the duration of the glow of the shock wave in the air gap. The glow arose at the instant of movement of the plate and stopped when it struck a Plexiglas obstacle installed at a distance of 6-8 mm from the investigated specimen. The conversion from the travel velocity of the aluminum plates to the mass velocities behind the shock front was accomplished by means of special calibration experiments in which we measured the velocity of the plates acquired under the effect of shock waves of known amplitude.

In all, we conducted three series of experiments, each of which consisted of 20-25 experiments. The results of the experiments are presented in Figs. 3-5 as a function of the path of attenuation referred to the thickness of the striking plate, which in all experiments was 1.5 mm. Data published earlier in [1] are marked by triangles in Fig. 3. The first two graphs illustrate the results obtained on steel specimens at initial pressures of 1.85 and 1.11 Mbar, and the third graph the data of measurements taken on copper at a collision pressure of 1.22 Mbar. On each attenuation curve we clearly see the place of arrival (marked by an arrow) of the unloading wave at the trajectory of the shock wave and the decrease of the mass velocity caused by it. The attenuation curves calculated in a hydrostatic approximation without consideration of strength effects and longitudinal expansion waves are shown by a dashed line in the graphs.

To change from mass velocities to shock-wave pressures, we used the laws of conservation and the D–U relations [11] (the values of velocities here and henceforth are given in km/sec)

$$D = 3.85 + 1.615U \tag{2.2}$$

$$D = 3.95 + 1.50U \tag{2.3}$$

which generalize the results of numerous previously published experiments (see references in [8]).

The results of treating the experimental data are presented in Table 1. Here for each series of experiments are given the initial parameters of the shock waves, i.e., their wave D and mass U velocities, pressures p_n, relative compressions of the material ρ/ρ_0, estimated temperatures T, pressure drops Δp_n in the unloading elastic wave obtained in experiments, relative distances of the first overtakings l_e/Δ, and the velocities of the elastic waves C_e calculated from Eq. (2.1).

3. Elastoplastic Parameters of Iron and Copper at Higher Pressures and Temperatures of Shock-Wave Compression. The next step necessary for reaching the final goals of the investigation was to determine the bulk moduli K_S by Eq. (1.6). The Gruneisen parameters figuring in Eq. (1.6) were found by two methods – from the experimental data on the compressibility of solid and porous specimens [11, 12]

TABLE 2

p_n, Mbar	Metal	γ	K_H, Mbar	K_S, Mbar	K_e, Mbar	G, Mbar	δ	Y_e, kbar
1.85	Fe	1.41	12.34	9.30±0.30 (8.91)	11.20±0.40	1.45±0.35	0.425±0.02	27±7
1.11	Fe	1.46	7.56	6.20±0.25 (6.60)	7.57±0.30	1.04±0.30	0.420±0.02	11±4
1.22	Cu	1.70	7.56	6.01±0.25	7.63±0.30	1.21±0.30	0.405±0.02	16±4

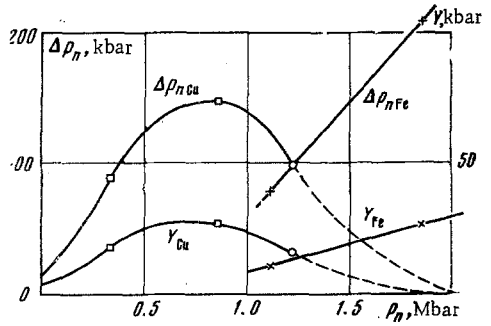

Fig. 7

and from the equations of state of iron and copper from [13]. The values of γ used for the initial states of shock-wave compression are given in Table 2. The slopes of K_H of the shock adiabatic curves for their unloaded states calculated by Eq. (1.8) with the use of parameters C_0 and λ from (2.2) and (2.3) are given there also. The calculated moduli K_S are compared in Table 2 with the moduli of one-dimensional elastic compression $K_e = \rho C_e^2$ found from the values of C_e in Table 1 and shear moduli $G = {}^3/_4(K_e - K_S)$. The table presents Poisson's ratio σ and yield strength Y calculated by (1.5) and (1.3) and from the experimental values of Δp_n. Along with the values of K_S the table contains, in parentheses, the bulk moduli found experimentally in [1] by measuring the plastic sound velocity by the overtaking unloading method. To eliminate the distorting effect of the leading elastic wave in [1], the states of the shock wave were recorded in the region of strong attenuation, at sections of its trajectory remote from the place of the first overtaking.

We will examine more thoroughly the effect of pressures and temperatures on the elastic characteristics of a metal with reference to copper, which does not experience phase transitions.

In Fig. 6 the values of the investigated parameters are presented as a function of shock-wave compression pressures. The moduli K_S, K_e, and G are given in a logarithmic scale and Poisson's ratio σ in a linear. The bulk modulus in the solid-state region represents a monotonically increasing function of pressure. Its values calculated by Eq. (1.6) agree satisfactorily with the data in [1] (dotted line). For the modulus of one-dimensional deformation K_e we know its initial value, value at p = 400 kbar from [1] (triangle), and value at p = 1.200 Mbar (circle) found in this investigation. The convergence of moduli K_S and K_e indicates, as follows from Eq. (1.5), a considerable increase of Poisson's ratio from 0.34 to 0.40 with increase of pressure. A slower increase of the shear modulus G in comparison with K_S and K_e is a consequence of this effect.

At a pressure of 2.05 Mbar melting occurs in shock-compressed copper, according to [14]. As for any fluid, here the effective values are $G = 0$, $\sigma = 0.5$, and $K_e = K_S$ as a consequence of the decrease of yield strength to zero. The sections of the curves interpolated to these values shown in Fig. 6 by a dot-dash line correspond to states with thermal relaxation times of tangential stresses comparable with the characteristic deformation times. The probable true values of the elastic parameters undistorted by relaxation phenomena are given in Fig. 6 by dashed curves.

The evolution of the strength characteristics of the investigated metals is shown in Fig. 7 as functions $\Delta p_n(p_n)$ and $Y(p_n)$. In addition to the data of the present study (circles) Fig. 7 also shows the results of measurements obtained in [6] (squares).*

The experimental values of Δp_n and Y are located on both sides of the maximum at $p \sim 800$ kbar. The approximately drawn descending branches of these functions touch the x axis at a melting pressure of 2.05 Mbar. The data for iron (crosses) lie on the ascending branches of their curves.

We will estimate for the value $\alpha = {}^2/_3 Y/p_n$ the degree of the nonhydrostatic character of the states occurring behind the shock front. For iron $\alpha = 1\%$ at $p_n = 1.85$ Mbar and $\alpha = 0.7\%$ at $p_n = 1.1$ Mbar. For cop-

*In [6] the change by means of Eq. (1.3) from the experimental Δp_n to Y was done at a constant $\sigma = 0.34$. The values of Y shown in Fig. 7 for 340 and 860 kbar were calculated on the basis of increased σ corresponding to the graph in Fig. 6. The converted Y are respectively 24 and 35% less than the values published in [6].

per $\alpha = 0.8\%$ at $p_n = 1.22$ Mbar. These slight deviations nevertheless have a considerable effect on expansion processes of shock-compressed metals – as the results of this study showed, the relative decrease of Δp_n of shock-wave compression pressures in the leading unloading elastic wave reaches 10%. In absolute value the recorded dynamic yield strengths exceed their values for normal conditions by a factor of 5-7.

LITERATURE CITED

1. L. V. Al'tshuler, S. B. Kormer, M. I. Brazhnik, L. A. Vladimirov, M. P. Speranskaya, and A. I. Funtikov, "Isentropic compressibility of aluminum, copper, lead, and iron at high pressures," Zh. Éksperim. i Teor. Fiz., 38, No. 4 (1960).
2. G. R. Fowles, "Shock wave compression of hardened and annealed 2024 aluminum," J. Appl. Phys., 32, No. 8 (1961).
3. D. R. Curran, "Nonhydrodynamic attenuation of shock waves in aluminum," J. Appl. Phys., 34, No. 9 (1963).
4. J. O. Erkman and A. B. Christensen, "Attenuation of shock waves in aluminum," J. Appl. Phys., 38, No. 13 (1967).
5. A. S. Kusubov and M. van Thiel, "Dynamic yield strength of 2024-T4 aluminum at 313 kbar," J. Appl. Phys., 40, No. 2 (1969).
6. S. A. Novikov and L. M. Sinitsyn, "Effect of shock-wave compression pressure on the magnitude of critical stresses in metals," Zh. Prikl. Mekhan. i Tekh. Fiz., No. 6 (1970).
7. L. W. Morland, "The propagation of plane irrotational waves through an elastoplastic medium," Phil. Trans. Roy. Soc. London, Ser. A., 251, No. 997 (1959).
8. L. V. Al'tshuler, "Use of shock waves in high-pressure physics," Usp. Fiz. Nauk, 85, No. 2 (1956).
9. K. K. Krupnikov, M. I. Brazhnik, and V. P. Krupnikova, "Shock wave compression of porous tungsten," Zh. Éksperim. i Teor. Fiz., 42, No. 3 (1962).
10. L. V. Al'tshuler, A. A. Bakanova, and I. P. Dudoladov, "Effect of electronic structure on compressibility of metals at high pressures," Zh. Éksperim. i Teor. Fiz., 53, No. 6 (1967).
11. L. V. Al'tshuler, K. K. Krupnikov, B. N. Ledenev, V. I. Zhuchikhin, and M. I. Brazhnik, "Dynamic compressibility and equation of state of iron at high pressures," Zh. Éksperim. i Teor. Fiz., 34, No. 4 (1958).
12. S. B. Kormer, A. I. Funtikov, V. D. Urlin, and A. N. Kolesnikova, Dynamic compression of porous metals and equation of state with variable heat capacity at high temperatures," Zh. Éksperim. i Teor. Fiz., 42, No. 3 (1962).
13. L. V. Al'tshuler, A. A. Bakanova, and R. F. Trunin, "Shock adiabatic curves and zero isotherms of seven metals at high pressures," Zh. Éksperim. i Teor. Fiz., 42, No. 1 (1962).
14. V. D. Urlin, "Melting at superhigh pressures obtained in a shock wave," Zh. Éksperim i Teor. Fiz., 49, No. 2 (1965).